

Antineoplastic Agents. 522. *Hernandia peltata* (Malaysia) and *Hernandia nymphaeifolia* (Republic of Maldives)^{1,1}

George R. Pettit,* Yanhui Meng, R. Patrick Gearing, Delbert L. Herald, Robin K. Pettit, Dennis L. Doubek, Jean-Charles Chapuis, and Larry P. Tackett

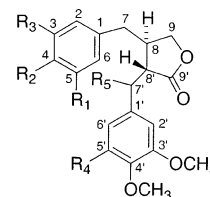
Cancer Research Institute and Department of Chemistry and Biochemistry, Arizona State University, Tempe, Arizona 85287-2404

Received March 21, 2003

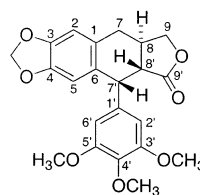
Bioassay (P388 lymphocytic leukemia cell line and human tumor cell lines)-guided separation of the extracts prepared from the tropical and coastal trees *Hernandia peltata* (Malaysia) and *Hernandia nymphaeifolia* (Republic of Maldives) led to the isolation of a new lignan designated as hernanol (**1**) and 12 previously known lignans: (–)-deoxypodophyllotoxin (**2**), deoxypicropodophyllin (**3**), (+)-epiaschantin (**4**), (+)-epieudesmin (**5**), praderin (**6**), 5'-methoxyxatein (**7**), podorhizol (**8**), deoxypodorhizone (**9**), bursehernin (**10**), kusunokinol (**11**), clusin (**12**), and (–)-maculatin (**13**). The oxidative cyclization (with VOF₃) of lignans **8**, **9**, and **10** resulted in a new and unusual benzopyran (**14**), isostegane (**15**), and a new dibenzocyclooctadiene lactone (**16**), respectively. The structure and relative stereochemistry of hernanol (**1**) and lignans **3**, **7**, **8**, **9**, **10**, **11**, and **12** were determined by 1D and 2DNMR and HRMS analyses. The structures and absolute stereochemistry of structures **2**, **4**, **5**, **6**, **13**, **14**, **15**, and **16** were unequivocally determined by single-crystal X-ray diffraction analyses. Evaluation against the murine P388 lymphocytic leukemia cell line and human tumor cell lines showed podophyllotoxin derivatives **2** and **3** to be strong cancer cell line growth inhibitors and substances **4**, **5**, **8**, and **15** to have marginal cancer cell line inhibitory activities. Seven of the lignans and one of the synthetic modifications (**14**) inhibited growth of the pathogenic bacterium *Neisseria gonorrhoeae*.

The tropical and relatively small (~54 species) plant family Hernandiaceae of trees, shrubs, and vines is divided among three genera. The largest, *Hernandia*, has some 24 species. References to the possible use of *H. ovigera* and *H. sonora* in traditional medicine for cancer treatment first appeared in a European medicinal plant treatise of 1831–1836.^{2a} Subsequent chemical investigations of *H. ovigera*^{2b–g} and *H. sonora*^{2h} (believed to correspond²ⁱ to *H. nymphaeifolia*^{2j–n}) have provided a good basis for these historical observations. Both species have been found to contain cancer cell growth inhibitory lignans, aporphine alkaloids, and podophyllotoxins.^{2h,n} To further explore the anticancer constituents of *H. nymphaeifolia* (Presl.) Kubitzki, we collected (in 1989) this plant in a new location, the Republic of the Maldives. For the same purpose, we collected *H. peltata* Meissner, which also may correspond to *H. sonora*, on the east coast of Malaysia in 1990.

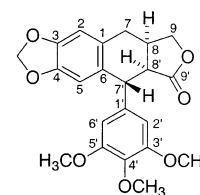
Both *H. nymphaeifolia* and *H. peltata* are common coastal trees that grow to 12–20 m in height and occur widely in tropical countries of Southeast Asia and Indo-pacific regions. *H. ovigera* and *H. peltata* have been used widely, for example, in Western Samoa,²ⁱ as a traditional medicine for boils, cough, diarrhea, abdominal pains, anticonvulsive treatment, eye problems, and a number of other indications that appear to include anticancer, antiviral, and antiparasite. In our present investigation we isolated and characterized eight previously known lignans (**2**,³ **3**,⁴ **4**,⁵ **5**,⁶ **6**,⁷ **7**,⁸ **8**,⁹ and **10**^{10,11}) from *H. peltata*. Similarly, nine known lignans (**2**,³ **3**,⁴ **5**,⁶ **8**,⁹ **9**,¹² **10**,^{10,11} **11**,¹³ **12**,¹⁴ and **13**¹⁵) were isolated from *H. nymphaeifolia*, together with one new lignan, an epitaxillagenin designated hernanol (**1**). The X-ray crystal structure (and absolute stereochemistry) of deoxypodophyllotoxin **2** (also



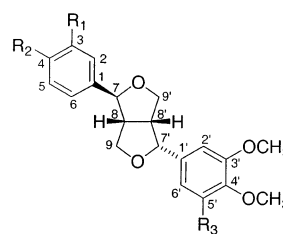
- 1, R₁ = R₅ = H, R₂ = OH, R₃ = R₄ = OCH₃ (hernanol)
 7, R₁ = R₄ = OCH₃; R₂, R₃ = OCH₂O; R₅ = H
 8, R₁ = H; R₂, R₃ = OCH₂O; R₄ = OCH₃; R₅ = OH
 9, R₁ = R₅ = H; R₂, R₃ = OCH₂O; R₄ = OCH₃
 10, R₁ = R₄ = R₅ = H; R₂, R₃ = OCH₂O
 13, R₁ = R₄ = R₅ = H, R₂ = R₃ = OCH₃



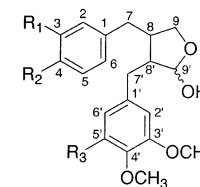
2



3



- 4, R₁, R₂ = OCH₂O; R₃ = OCH₃
 5, R₁ = R₂ = OCH₃, R₃ = H
 6, R₁ = R₃ = OCH₃, R₂ = OH



- 11, R₁ = R₂ = OCH₃, R₃ = H
 12, R₁, R₂ = OCH₂O; R₃ = OCH₃

¹ Dedicated to the late Dr. Monroe E. Wall and to Dr. Mansukh C. Wani of Research Triangle Institute for their pioneering work on bioactive natural products.

* To whom correspondence should be addressed. Tel: 480-965-3351. Fax: 480-965-8558. E-mail: bpettit@asu.edu.

known as anthricin) has been reported¹⁶ and has served as a template in the conformational analysis and confor-

Table 1. ^1H and ^{13}C NMR Assignments for Hernanol (**1**) in CHCl_3^a

position	$\delta^1\text{H}$	$^1\text{H} - ^1\text{H}$ COSY	$\delta^{13}\text{C}$	HMBC ^b
1			129.7	H-5, H-7a, b, H-8(w)
1'			133.4	H-7', H-8', H-2'(w), H-6'(w)
2	6.44s (1H)		110.9	H-6, H-7
2'	6.34s (1H)		106.3	H-6', H-7'
3			146.6	OCH_3 -3, OH-4, H-2, H-5
3'			153.3	OCH_3 -3', H-2'
4			144.5	OH-4, H-2, H-5, H-6
4'			136.9	OCH_3 -4', H-2', H-6'
5	6.82d (1H, $J = 7.5$ Hz)	H-6	114.5	OH-4
5'			153.3	OCH_3 -5', H-6'
6	6.53d (1H, $J = 7.5$ Hz)	H-5	121.3	H-2, H-7a, b
6'	6.34s (1H)		106.3	H-2', H-7'
7	2.65dd (1H, $J = 13.5, 6.5$ Hz, H-7a) 2.56dd (1H, $J = 13.5, 8.5$ Hz, H-7b)	H-7b, H-8 H-7a, H-8	38.3	H-2, H-6, H-8, H-8', H-9a, H-9b(w)
7'	2.92m (1H)	H-8'	35.2	H-2', H-6', H-8, H-8'
8	2.48m (1H)	H-7a,b, H-8', H-9,	41.1	H-7ab, H-7', H-9a, b(w)
8'	2.60m (1H)	H-7', H-8	46.5	H-7, H-7', H-8, H-9b(w)
9	3.89t (1H, $J = 8.5$ Hz, H-9a) 4.19dd (1H, $J = 8.5, 7.5$ Hz, H-9b)	H-9b, H-8 H-9a, H-8	71.3	H-7, H-8
9'			178.6	H-7', H-8', H-9a,b
OCH_3 -3	3.81s (3H)		55.8	
OCH_3 -3'	3.81s (3H)		56.1	
OH-4	5.51s (1H)			
OCH_3 -4'	3.82s (3H)		60.9	
OCH_3 -5'	3.81s (3H)		56.1	

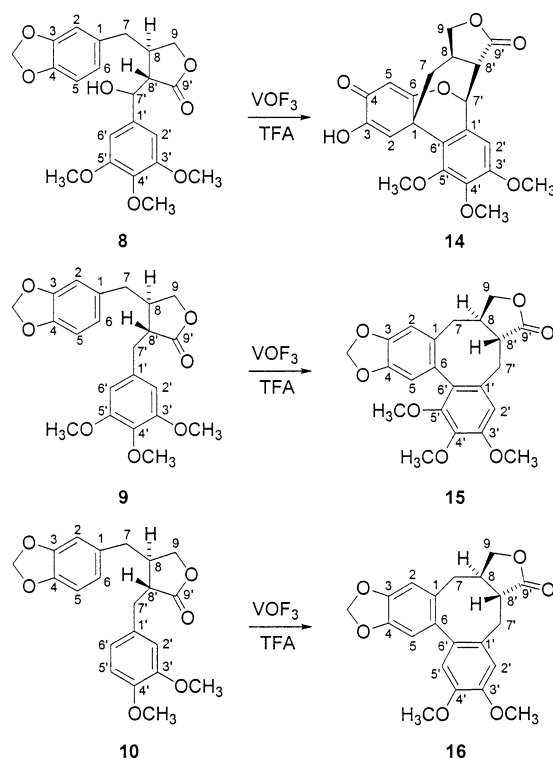
^a Measured at 500 MHz. ^b w = weak.

mational–biological activity relationships of other podophyllotoxin analogues.^{16,17} The absolute structure of the lignan **15** (known as isostegane and here produced by semisynthesis as described below) has also been determined, on the basis of X-ray structural analysis of the (+)-12-bromo derivative of isostegane.¹⁸ Some (**3**, **6**, **11**, **12**, and **13**) were not previously known to occur in these two *Hernandia* species. Another objective of this research was to employ several of the more abundant lignans for synthetic conversion to cyclic biaryls with the prospect of obtaining new cancer cell growth inhibitors related to podophyllotoxin. For that purpose, oxidative cyclization of lignans **8**, **9**, and **10** with VOF_3 ¹⁹ yielded the unusual benzopyran **14**, isostegane (**15**),¹⁹ and a new dibenzocyclooctadiene lactone (**16**), respectively. Herein we report the structural elucidation, as well as the anticancer and antimicrobial evaluations, of these 16 *Hernandia* constituents and structural modifications.

Results and Discussion

The initial CH_2Cl_2 – CH_3OH (1:1) extracts of *H. nymphaeifolia* and *H. peltata* were separately partitioned between CH_3OH – H_2O (9:1 \rightarrow 1:1) and hexane \rightarrow CH_2Cl_2 . Bioassay-guided (P388 lymphocytic leukemia cell line) separation of the CH_2Cl_2 fraction from each of the *Hernandia* species solvent partitioning sequences by a series of Sephadex LH-20 column chromatographic steps followed by final purification employing HPLC and recrystallization led to the new lignan hernalol (**1**, 6.5×10^{-4} % yield from *H. nymphaeifolia*) and 12 known lignans (**2**–**13**).

The hernalol (**1**) molecular formula was assigned as $\text{C}_{22}\text{H}_{26}\text{O}_7$ on the basis of high-resolution APCI⁺ mass spectroscopy ($[\text{M} + 1]^+$ at m/z 403). The infrared absorption at 1769 cm^{-1} ($\text{C}=\text{O}$) and the appearance of signals at δ 2.48, 2.60 (2H, m, C8,8'-H), 2.56, 2.65, and 2.92 (4H, m C7,7'-H), and 3.89, 4.19 (2H, each dd, C9-H) in the ^1H NMR spectrum (Table 1) suggested a 2,3-dibenzylbutyrolactone-type lignan. The ^1H NMR spectrum of hernalol (**1**) also revealed five aromatic proton signals at δ 6.44 (1H, s), 6.53 (1H, d, $J = 7.5$ Hz), 6.82 (1H, d, $J = 7.5$ Hz), and 6.34 (2H, s). The splitting pattern and coupling constants of the five



proton signals confirmed their origin from a trisubstituted and a tetrasubstituted benzene ring. The ^1H – ^1H COSY spectrum (Table 1) confirmed the connection of four saturated carbon atoms in the butyrolactone ring and also confirmed the connection of C-7 to C-8 and C-7' to C-8'. These assignments were further defined by HMQC and HMBC spectra (Table 1), confirming the presence of 3-methoxy-4-hydroxybenzyl and 3',4',5'-trimethoxybenzyl groups. In addition, the bonding of the 3-methoxy-4-hydroxybenzyl group to lactone position C-7 and the 3,4,5-trimethoxybenzyl group to C-7' was established by the strong correlations observed from H-7_{a,b} (δ 2.65, 2.56) to C-1 (129.7) and from H-7' (δ 2.92) to C-1' (133.4). Thus, the structure of hernalol (**1**) was determined unambiguously.

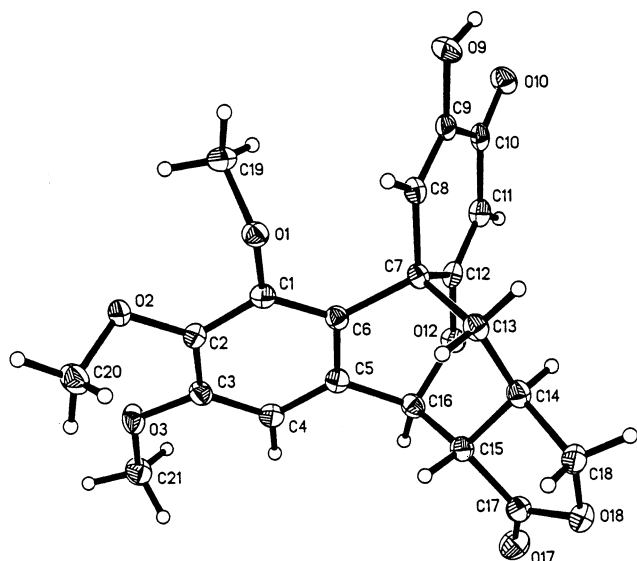


Figure 1. X-ray crystal structure of benzopyran **14** with 50% probability thermal ellipsoids.

The relative stereochemistry of the two chiral carbons in hernanol (**1**) was deduced as $8R^*$, $8'R^*$ on the basis of comparing their carbon chemical shifts with those of known lignans **7**, **9**, and **10**, whose relative stereochemistry has already been determined as $8R^*$, $8'R^*$, and especially with lignan **13**, whose absolute stereochemistry has already been decided by single-crystal X-ray analysis. The *trans*-relationship of the C-8 and C-8' protons of the known 2,3-dibenzylbutyrolactone lignans **7**, **8**, **9**, **10**, and **13** isolated from *H. nymphaeifolia* suggests that they might be derived from analogous biosyntheses. Interestingly, when comparing the ^1H and ^{13}C NMR chemical shifts of hernanol (**1**) with those of traxillagenin^{20,21} (first isolated from the stems of *Trachelospermum asiaticum*²¹ and its structure deduced on the basis of ^{13}C NMR and MS data), it was found that the carbon chemical shifts of the two compounds are very similar (less than 0.8 ppm difference). Because the stereochemistry of hernanol (**1**) was established by HMBC, it is likely that the traxillagenin structure needs to be reassigned to that of lignan **1**. The structures and relative stereochemistry of lignans **3**, **7**, **8**, **9**, **10**, **11**, and **12** were determined by 1D and 2D NMR and HRMS analyses as well as by comparison with published data.^{4,8-14} The structures of compounds **2**, **4-6**, and **13-16** were determined by single-crystal X-ray diffraction techniques. For a majority of these compounds, due to the high oxygen content, anomalous dispersion effects were sufficiently intense as to allow determination of the absolute stereochemistry. Thus, refinement of the absolute structure (Flack parameter) in the cases of compounds **2**, **4**, **6**, and **13-16** allowed conclusive assignment of their absolute stereochemical structures.

X-ray structure determinations of compounds **2**, **4-6**, **13**, and **15** confirmed the structures of these known compounds as deoxypodophyllotoxin, (+)-epiashantin, (+)-epieudesmin, praderin, maculatin, and isostegane, respectively. Figures and X-ray tables for these known compounds are summarized in the Supporting Information. The absolute stereochemical structures of the remaining substances **14-16** (Figures 1-3 respectively), which were isolated via synthetic modifications, are presented below.

All of the X-ray data collections were performed at -150°C (123 K) on a Bruker SMART 6000 X-ray diffractometer using Cu radiation and a graphite monochromator. Suitable crystals, obtained via crystallization methods, were

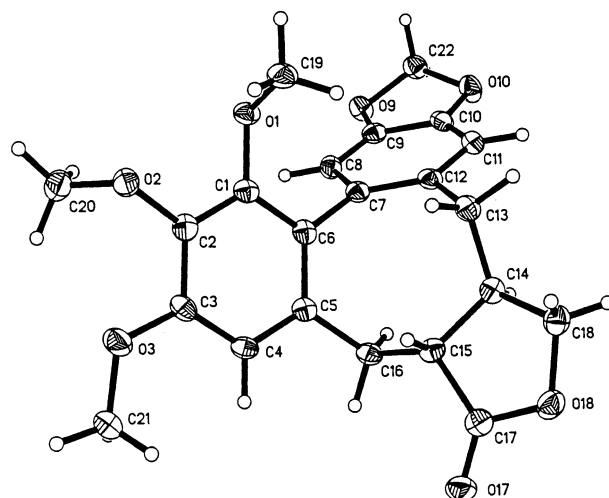


Figure 2. X-ray structure of isostegane **15** with 50% thermal probability ellipsoids.

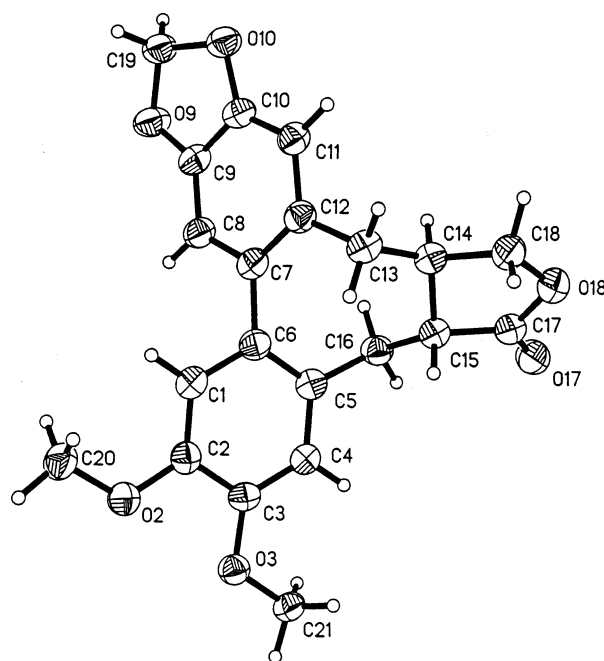


Figure 3. X-ray structure of deoxyisostegane **16** with 50% thermal probability ellipsoids.

mounted on the tip of a glass fiber with Vaseline and frozen into position with a cooled N_2 gas stream, and data collection was initiated. Frames of data were collected such as to survey a complete sphere of reflections with at least $>95\%$ coverage of the total number of theoretical reflections possible. Structure solution and refinement were performed with the Bruker SHELXTL²² software package. In this manner, unambiguous structure determinations were obtained for the known compounds **2**, **4-6**, and **13**. Absolute stereochemical structures were also determined for the reaction products **14-16** (Figures 1-3), obtained from the corresponding reaction of **8-10** with VOF_3 ,¹⁹ as described below.²³

A series of oxidative coupling methods using heavy metal oxidants^{19,24} has been used to synthesize stegane and isostegane lignans from *cis*- or *trans*-3,4-dibenzylbutyrolactones. As a part of our continuing efforts to discover useful anticancer agents, cyclization of podorhizol (**8**), deoxypodorhizone (**9**), and bursehernin (**10**) was conducted by treating each with VOF_3 .¹⁹ As expected, isostegane (**15**, 14% yield) and a new deoxy isostegane (**16**, 20%

Table 2. Murine P388 Lymphocytic Leukemia Cell Line and Human Cancer Cell Line Inhibition Values (ED₅₀ expressed in μg/mL) for Lignans **2**, **3**, **4**, **5**, **8**, and **15**^a

cancer cell line ^b	2	3	4	5	8	15
P388	0.0023	0.030	1.5	1.7	>1.0	6.1
BXPC-3	0.0029	0.061	>10	3.4	3.8	4.7
MCF-7	0.0021	0.026	>10	3.5	6.6	4.3
SF268	0.0033	0.041	>10	3.8	>10	4.9
NCI-H460	0.0027	0.067	>10	3.8	>10	5.8
KM20L2	0.0028	0.054	>10	3.0	>10	4.8
DU-145	0.0028	0.051	>10	3.1	>10	5.3

^a In DMSO. ^b Cancer cell type (P388, lymphocytic leukemia; BXPC-3, pancreas adenocarcinoma; MCF-7, breast adenocarcinoma; SF268, CNS glioblastoma; NCI-H460, lung large cell; KM20L2, colon adenocarcinoma; DU-145, prostate carcinoma).

yield) were synthesized from deoxypodorhizone (**9**) and bursehernin (**10**), respectively. However, the cyclization of podorhizol (**8**) resulted in an unusual benzopyran (**14**, 42% yield), instead of the expected isostegane-type product. In this respect, an *O*-benzoquinone was formed following cleavage of its methylenedioxy group when isostegane was treated with thallium(III) oxide in TGA.²⁴ Each product was purified by a flash chromatography, HPLC, and recrystallization sequence. Colorless crystals of each were obtained, and their structures and absolute stereochemistry were determined by X-ray diffraction analyses.

The X-ray structure of the new, unusual benzopyran product **14** is shown in Figure 1. Both inter- and intramolecular H-bonding were observed between the hydroxyl hydrogen and the carbonyl oxygen in the cyclohexadienone ring in this compound. In contrast to the rather complex and unique ring formation exemplified by **14**, the cyclization of lactones **9** and **10** took a more normal course of closure, forming the eight-membered rings of **15** and **16**, respectively, as shown in Figures 2 and 3.

All thirteen lignans (**1–13**) isolated from *H. nymphaeifolia* and *H. peltata* and the three synthetic modifications (**14–16**) were examined using the murine P388 lymphocytic leukemia cell line and a selection of human cancer cell lines. Six lignans (**2–5**, **8**, and **15**) exhibited cancer cell growth inhibitory activities ranging from potent to marginal (Table 2). Among the six lignans, deoxypodophyllotoxin (**2**), which is known as an anticancer agent,^{25–27} shows the strongest activity in both P388 and human cancer lines, while (+)-epiaschantin (**4**) shows activity only in the P388 leukemia cell line and podorhizol (**8**) is active in only two types of human cell lines. The other 10 lignans were inactive in both the P388 and human tumor cell lines. Antimicrobial susceptibility testing was performed by the reference broth microdilution assay.^{28,29} Lignans **1–3**, **8**, **11–13**, and synthetic modification **14** inhibited growth of the Gram-negative pathogen *Neisseria gonorrhoeae* (minimum inhibitory concentrations 32–64 μg/mL). Lignan **9** was not available for antimicrobial evaluation.

In conclusion, this detailed bioassay-directed investigation of *H. nymphaeifolia* and *H. peltata* has resulted in a more definitive understanding of the lignan-type anticancer constituents. In parallel, the structures of five lignans and three oxidative cyclization products were established unequivocally by X-ray crystal structure determination. These X-ray crystal structures will now provide a sound reference point for structure determinations of related compounds by spectral methods.

Experimental Section

General Experimental Methods. All chromatographic solvents were redistilled. Sephadex LH-20 used for partition column chromatography was obtained from Pharmacia Fine

Chemicals AB. Semipreparative HPLC was performed with a Gilson model 805 HPLC coupled with a Gilson model 117 UV detector. Analytical HPLC was conducted with a Hewlett-Packard model 1050 HPLC coupled with a Hewlett-Packard diode-array detector. Melting points were measured on an Olympus electrothermal melting point apparatus and are uncorrected. The optical rotation measurements were recorded with a Perkin-Elmer 241 polarimeter. UV spectra were collected with a Perkin-Elmer Lambda 3B UV/vis spectrometer. The IR spectra were recorded with a Thermo Nicolet Avatar 360 infrared spectrometer. NMR spectra were determined with a Varian XL-300 or a Varian UNITY INOVA-500 and 400 spectrometer using tetramethylsilane (TMS) as an internal reference. High-resolution mass spectra were obtained using a JEOL LCMate magnetic sector instrument in either the FAB mode with a glycerol matrix or by APCI with a poly(ethylene glycol) reference.

***Hernandia nymphaeifolia*.** On March 28, 1989, this tree (~15 m) was collected on the small island of Guradu in the South Male Atoll, Republic of Maldives, and preserved in absolute ethanol. Later in 1989, four 55 gal drums of the tree (bark, stems, and leaves) were collected and 40 L of absolute ethanol was added to each drum. Our procedure avoided the problems (e.g., fungal overgrowth) associated with large-scale plant drying in remote tropical areas and long shipment times. The taxonomic identification was undertaken (by Drs. D. H. Lorence and L. R. Landrum), and a voucher specimen is maintained in our institute.

***Hernandia peltata*.** The initial collection of this tree (~1 kg sample) was performed on September 9, 1990, at Pulau Redang, on the east coast of Malaysia. The collected material was preserved in MeOH and identified, and a voucher specimen was stored as noted above for *H. nymphaeifolia*.

Extraction and Initial Separation of *H. nymphaeifolia* and *H. peltata* Constituents. Approximately 1000 kg of *H. nymphaeifolia* was extracted (2×; 10, 5 days) using 1:1 CH₂Cl₂–CH₃OH. After each extraction, 30% by volume of H₂O was added to separate a CH₂Cl₂ fraction, yielding 1329 and 316 g, respectively. A 610 g aliquot of the first CH₂Cl₂ phase was partitioned between CH₃OH–H₂O (9:1 → 1:1) and hexane (for the 9:1 mix) followed by CH₂Cl₂ (for the 1:1), which provided 282 g of a (P388 ED₅₀ 0.034 μg/mL) CH₂Cl₂ fraction. The solvent partitioning sequence was a modification of the original procedure of Bligh and Dyer.³⁰ By applying the same partitioning procedure, 39.6 g of a CH₂Cl₂–CH₃OH extract of *H. peltata* was partitioned between CH₃OH–H₂O (9:1 → 3:2) and hexane (for the 9:1 mix) followed by CH₂Cl₂ (for the 3:2), affording 7.3 g of a P388 active CH₂Cl₂ fraction (P388 ED₅₀ 0.022 μg/mL).

Separation of the Methylene Chloride Fraction from *H. nymphaeifolia*. The CH₂Cl₂ fraction was passed through a Sephadex LH-20 column with CH₃OH as eluent. Three P388 active fractions were obtained, and each was chromatographed on a column of Sephadex LH-20 using CH₃OH–CH₂Cl₂ (2:3) as eluent. Again, three P388 active fractions (*a*, *b*, and *c*) were obtained. Fractions *a* and *b* were combined and subjected to separation on a Sephadex LH-20 column, using hexane–toluene–CH₃OH (3:1:1) as eluent, leading to three distinct compounds and three P388 active fractions (*d*, *e*, and *f*). The three nearly pure products were recrystallized (2×) from CH₃OH. Three pure lignans, **2** (colorless needles, 1.98 g), **3** (colorless needles, 0.86 g), and **5** (colorless needles, 0.90 g), were obtained. Fraction *d* was first separated on a Sephadex LH-20 column, using 2-propanol–toluene–hexane (1:1:3) as eluent, and then further separated on a silica gel column, using CH₂Cl₂–EtOAc–hexane (3:1:1) as eluent. A pure colorless semisolid (**10**) (0.39 g) and two other pure white solids were obtained. Recrystallization (2×) of the two white solids from CH₃OH resulted in **13** (colorless planar crystals, 14.5 mg) and **9** (colorless needles, 0.285 g). Fraction *e* was first separated on a column of Sephadex LH-20, using 2-propanol–toluene–hexane (1:1:3) as eluent, followed by separation on a silica gel column, using EtOAc–hexane (1:1) as eluent. One pure lignan (**8**) (colorless semisolid, 0.10 g) and another nearly pure

fraction were obtained. The latter fraction was purified by semipreparative HPLC using a SphereClone ODS(2) column and a gradient mobile phase (30% CH₃CN in H₂O for 60 min at a flow rate of 2.8 mL/min) to afford 4.0 mg of hernalol (**1**) (colorless semisolid): $[\alpha]_D^{24} -36.2^\circ$ (*c* 0.26, CH₃OH); UV λ_{max} (CH₃OH) (log ϵ) 203 (5.0), 225 (4.5), 278 (3.8) nm; ¹H and ¹³C NMR (Table 1); HRAPCI MS (positive-ion mode) *m/z* 403.175 [M + H]⁺ (calcd for C₂₂H₂₆O₇, 402.4376).

The purification of fraction *f*, first on a Sephadex LH-20 column, using 2-propanol–toluene–hexane (1:1:3) as eluent, and then by analytical HPLC using a Zorbax C₁₈ column with an isocratic mobile phase (41% CH₃CN in H₂O at a flow rate of 1 mL/min), yielded **11** (small colorless needles, 2.8 mg). Fraction *c* was separated on a silica gel column, using CH₂Cl₂–EtOAc–hexane (3:1:1) as eluent, and one nearly pure fraction was obtained which was recrystallized (2×) from CH₃OH to provide **12** (small colorless needles, 10.8 mg).

Separation of the Methylene Chloride Fraction from *H. peltata*. A portion of the P388 active CH₂Cl₂ fraction (0.14 g) was chromatographed on a column of Sephadex LH-20, using CH₃OH as eluent. Again, three P388 active fractions (*a*, *b*, and *c*) were selected for further separation. Fractions *a* and *b* were both recrystallized (3×) from CH₃OH, to provide lignans **4** (colorless needles, 25 mg) and **5** (colorless needles, 9.8 mg). Separation of the mother liquid from recrystallization of lignan **4** was first conducted on a Sephadex LH-20 column, using toluene–CH₃OH–acetone–*n*-hexane (8:1:2:2) as eluent, and then by semipreparative HPLC using a LUNA 5 μ m C₁₈ column with an isocratic mobile phase (36% CH₃CN in H₂O at 2.8 mL/min), to give a pure compound and the nearly pure fraction *d*. The pure compound was recrystallized from MeOH (2×) to afford colorless prism crystals of lignan **2** (51 mg). Fraction *d* was further separated by semipreparative HPLC again, using a LUNA 5 μ m C₁₈ column and an isocratic mobile phase (37% CH₃CN in H₂O at 2.8 mL/min), leading to lignan **10** as a colorless semisolid (28 mg). The mother liquid from lignan **5** was further separated on a Sephadex LH-20 column using toluene–CH₃OH–hexane (5:1:1) as eluent and finally by semipreparative HPLC using a SYNERGI 4 μ m RP 80 A column and an isocratic mobile phase (36% CH₃CN in H₂O at a flow rate of 2.8 mL/min): the result was lignan **6** (colorless needles, 3.1 mg). Fraction *c* was passed through a Sephadex LH-20 column in CH₃OH and eluted in CH₃OH. A P388 active fraction was obtained. Separation of this fraction by semipreparative HPLC using a LUNA 5 μ m C₁₈ column and an isocratic mobile phase (40% CH₃CN in H₂O at a flow rate of 2.8 mL/min) afforded three P388 active fractions (*e*, *f*, and *g*). Fraction *e* was further separated by analytical HPLC using a SYNERGI 4 μ m RP 80 A column and isocratic mobile phase (34% CH₃CN in H₂O at 1 mL/min). Pure lignan **8** (colorless semisolid, 1.5 mg) was obtained. Fraction *f* was separated by semipreparative HPLC (2×) (first on a SYNERGI 4 μ m RP 80 A column with an isocratic mobile phase of 35% CH₃CN in H₂O at 2.8 mL/min and second on a Zorbax C₁₈ column with an isocratic mobile phase of 34% CH₃CN in H₂O at 4 mL/min). Pure lignan **7** (colorless semisolid, 2.1 mg) was obtained. The purification of fraction *g* by semipreparative HPLC using a SYNERGI 4 μ m RP 80 A column and an isocratic mobile phase of 34% CH₃CN in H₂O at a flow rate of 2.8 mL/min afforded lignan **3** (colorless needles, 5.2 mg).

Synthesis of Benzopyran 14. A solution of lignan **8** (0.103 g, 0.247 mmol in DCM 5 mL) was added dropwise to a solution of VOF₃ (91.8 mg, 0.741 mmol) in 2:1 TFA–DCM (3 mL) and TFA anhydride (0.1 mL) at –15 °C under argon. The reaction mixture was stirred at –15 °C for 4 h and the reaction terminated by addition of saturated NaHCO₃ (12 mL) and DCM (12 mL). The organic layer was separated, solvent removed in vacuo, and the residue subjected to flash chromatography, using EtOAc–CH₂Cl₂–hexane (1:1:3) as eluent, to provide pyran **14** (43 mg, 42%). Recrystallization from CH₃OH (2×) gave pure colorless planar crystals of pyran **14**: mp 218 °C (dec); $[\alpha]_D^{24} +38.6^\circ$ (*c* 0.22, CH₃OH); ¹H NMR (400 MHz in CDCl₃) δ (ppm) 2.13 (1H, t, *J* = 12.8 Hz, H-7a), 2.24 (1H, dd, *J* = 12.8, 4.8 Hz, H-7b), 2.45 (1H, d, *J* = 14.4 Hz, H-8'), 2.97 (1H, m, H-8), 3.82 (1H, dd, *J* = 11.2, 8.4 Hz, H-9a), 4.36

(1H, dd, *J* = 8.4, 6.4 Hz, H-9b), 5.67 (1H, s, H-7'), 5.97 (1H, s, H-5), 6.39 (1H, s, OH-3), 6.67 (1H, s, H-2'), 7.05 (1H, s, H-2), 3.88 (3H, s, OCH₃-3'), 3.84 (3H, s, OCH₃-4'), 3.78 (3H, s, OCH₃-5'); ¹³C NMR (400 MHz in CDCl₃) δ (ppm) 189.1 (C-4), 174.9 (C-6), 173.5 (C-9'), 153.6 (C-3'), 152.2 (C-5'), 143.6 (C-4'), 142.9 (C-3), 133.4 (C-1'), 120.1 (C-6'), 115.8 (C-2), 104.6 (C-5), 104.1 (C-2'), 75.0 (C-7'), 70.3 (C-9), 61.6 (OCH₃-5'), 60.9 (OCH₃-4'), 56.2 (OCH₃-3'), 49.1 (C-8'), 45.5 (C-1), 40.3 (C-7), 39.3 (C-8); HRAPCI MS (positive-ion mode) calcd for C₂₁H₂₀O₈ 400.38787, found, *m/z* 401.1236 [M + 1]⁺.

Crystal Structure of Benzopyran 14. A large, colorless block-shaped crystal, obtained via slow evaporation of a methanol solution, with approximate dimensions of 0.96 × 0.64 × 0.48 mm, was mounted on the tip of a glass fiber. An initial set of cell constants was calculated from reflections harvested from three sets of 60 frames at 123(1) K on a Bruker 6000 diffractometer at –150 °C. Cell parameters indicated an orthorhombic space group. A subsequent data collection, using 5 s scans/frame and 0.396° steps in ω , was conducted in such a manner as to completely survey a complete sphere of reflections. This resulted in >97.9% coverage of the total reflections possible to a resolution of 0.87 Å. A total of 13 520 reflections were harvested from the total data collection, and final cell constants were calculated from a set of 6377 reflections from these data. Subsequent statistical analysis of the complete reflection data set using the XPREP²² program indicated the space group was *P*2₁2₁2₁. Crystal data: C₂₁H₂₀O₈, *a* = 7.3608(1) Å, *b* = 11.0299(1) Å, *c* = 22.7788(3) Å, *V* = 1849.39(4) Å³, λ (Cu K α) = 1.54178 Å, μ (Cu K α) = 0.937 mm^{–1}, ρ_c = 1.438 g cm^{–3} for *Z* = 4 and *M_r* = 400.37, *F*(000) = 840. After data reduction, merging of equivalent reflections, and rejection of systematic absences, 3365 unique reflections remained (*R*_{int} = 0.0191), of which 3328 were considered observed [*I*_o > 2 σ (*I*_o)] and were used in the subsequent structure solution and refinement. An absorption correction was applied to the data with SADABS.³¹ Direct methods structure determination and refinement were accomplished with the SHELXTL NT ver. V6.12²² suite of programs. All non-hydrogen atom coordinates for lactone **14** were located using the default settings of that program. The remaining hydrogen atom coordinates were calculated at optimum positions using the program SHELXL.²² These latter atoms were assigned thermal parameters equal to either 1.2 or 1.5 (depending upon chemical type) of the *U*_{iso} value of the atom to which they were attached, and then both coordinates and thermal values were forced to ride that atom during the final cycles of refinement. All non-hydrogen atoms were refined anisotropically in a full-matrix least-squares refinement process. Both inter- and intramolecular hydrogen bonding (O-9 hydroxyl hydrogen and the O-10 carbonyl oxygen) was observed in the unit cell. The absolute structure parameter (Flack *x* parameter) = 0.0259 with an esd of 0.1130, indicating that the absolute structure shown in Figure 1 represents the correct enantiomer. The final standard residual *R*₁ value for the model shown in Figure 1 was 0.0268 (for observed data) and 0.0270 (for all data). The corresponding Sheldrick *R* values were *wR*₂ of 0.0697 and 0.0699, respectively. The goodness-of-fit factor was 1.052. The difference Fourier map showed insignificant residual electron density, the largest difference peak and hole being +0.209 and –0.234 e/Å³, respectively. The final bond distances and angles for the structural model, as shown in Figure 1, were all within acceptable limits.

Synthesis of Isostegane (15). The preceding reaction was repeated using lignan **9** (0.28 g, 0.69 mmol in DCM, 15 mL) and VOF₃ (0.25 g, 1.97 mmol in a 2:1 mixture of TFA–DCM (15 mL) and TFA anhydride (0.4 mL)). Isolation of the product (**15**) was performed using saturated NaHCO₃ (35 mL) and DCM (35 mL) followed by flash chromatography, using EtOAc–CH₂Cl₂–hexane (1:1:3) as noted above (**14**) to give 40 mg of isostegane (14% yield). Recrystallization (2×) from CH₃OH afforded colorless planar crystals: mp 169–171 °C; ¹H and ¹³C NMR data were the same as already published;³² EIMS calcd for C₂₂H₂₂O₇, 398.41, found *m/z* 398 [M]⁺.

Crystal Structure of Isostegane 15. A large, colorless plate, obtained via slow evaporation of a methanol solution,

with approximate dimensions of $0.6 \times 0.64 \times 0.16$ mm, was mounted on the tip of a glass fiber. Data collection, using 5 s scans/frame and 0.396° steps in ω , was conducted at 123(1) K on a Bruker 6000 diffractometer at -150°C . Cell parameters indicated a monoclinic space group. A total of 7003 reflections were harvested from the total data collection, and final cell constants were calculated from a set of 6682 reflections from these data. Subsequent statistical analysis of the complete reflection data set using the XPREP²² program indicated that the space group was $P2_1$. Crystal data: $\text{C}_{22}\text{H}_{22}\text{O}_7$, $a = 11.6304(2)$ Å, $b = 6.85900(10)$ Å, $c = 12.5499(2)$ Å, $V = 954.68(3)$ Å³, $\lambda = (\text{Cu K}\alpha) = 1.54178$ Å, $\mu(\text{Cu K}\alpha) = 0.863$ mm⁻¹, $\rho_c = 1.386$ g cm⁻³ for $Z = 2$ and $M_r = 398.40$, $F(000) = 420$. After data reduction, 2815 reflections were considered observed [$I_o > 2\sigma(I_o)$] and were used in the subsequent structure solution and refinement. An absorption correction was applied to the data with SADABS.³¹ Direct methods structure determination and refinement were accomplished with the SHELXTL NT ver. V6.12²² suite of programs. All non-hydrogen atom coordinates for isostegane (**15**) were located using the default settings of that program. The remaining hydrogen atom coordinates were calculated at optimum positions using the program SHELXL.²² These latter atoms were assigned thermal parameters equal to either 1.2 or 1.5 (depending upon chemical type) of the U_{iso} value of the atom to which they were attached, then both coordinates and thermal values were forced to ride that atom during the final cycles of refinement. All non-hydrogen atoms were refined anisotropically in a full-matrix least-squares refinement process. The absolute structure parameter (Flack x parameter) was also refined to a value of 0.0900 with an esd of 0.1600, indicating that the absolute structure shown in Figure 2 represents the correct enantiomer. The final standard residual R_1 value for the model shown in Figure 2 was 0.0353 (for observed data) and 0.0355 (for all data). The corresponding Sheldrick R values were wR_2 of 0.0941 and 0.0943, respectively. The goodness-of-fit factor was 1.043. The difference Fourier map showed insignificant residual electron density, the largest difference peak and hole being $+0.179$ and -0.240 e/Å³, respectively. The final bond distances and angles for the structural model, as shown in Figure 2, were all within acceptable limits.

Synthesis of Deoxyisostegane 16. When the above (**14**, **15**) oxidative cyclization reaction was applied to lignan **10** (0.39 g, 1.06 mmol in DCM, 20 mL) and VOF_3 (0.40 g, 3.19 mmol in 2:1 TFA–DCM (20 mL) and TFA anhydride (0.5 mL)), followed by the preceding (**15**) isolation procedure, 82 mg (20%) of lactone **16** was obtained. Two recrystallizations from CH_3OH yielded colorless planar crystals: mp $155\text{--}157^\circ\text{C}$; $[\alpha]_D^{24} +160.3^\circ$ (c 0.26, CH_3OH); $^1\text{H NMR}$ (300 MHz in CDCl_3) δ (ppm) 4.36 (1H, dd, $J = 8.1, 6.0$ Hz, H-9a), 3.77 (1H, dd, $J = 11.0, 8.1$ Hz, H-9b), 2.20 (1H, m, H-8), 2.38 (1H, d, $J = 8.7$ Hz, H-7a), 2.60 (1H, d, $J = 13.2$ Hz, H-7b), 2.15 (1H, m, H-8'), 3.14 (1H, d, $J = 13.2$ Hz, H-7'a), 2.28 (1H, d, $J = 8.7$ Hz, H-7'b), 5.96 (2H, d, $J = 4.5$ Hz, OCH_2O), 6.77 (1H, s, H-2'), 6.66 (1H, s, H-2), 6.65 (1H, s, H-5), 6.64 (1H, s, H-5'), 3.84 (1H, s, OCH_3 -4'), 3.90 (1H, s, OCH_3 -3'); $^{13}\text{C NMR}$ (400 MHz in CDCl_3) δ (ppm) 176.6 (C-9'), 148.9 (C-3'), 147.5 (C-4), 147.2 (C-3), 146.1 (C-4'), 132.1 (C-1'), 132.3 (C-6'), 132.4 (C-6), 133.5 (C-1), 113.9 (C-5'), 111.7 (C-2'), 111.1 (C-5), 108.8 (C-2), 101.3 (OCH_2O), 70.1 (C-9), 56.1 (OCH_3 -3'), 56.1 (OCH_3 -4'), 50.0 (C-8'), 47.0 (C-8), 34.3 (C-7), 32.1 (C-7'); HRAPCI MS (positive-ion mode) calcd for $\text{C}_{21}\text{H}_{20}\text{O}_6$ 368.3799, found m/z 369.

Crystal Structure of Deoxyisostegane 16. A colorless, block-shaped crystal, obtained via slow evaporation of a methanol solution, with approximate dimensions of $0.48 \times 0.48 \times 0.32$ mm, was mounted on the tip of a glass fiber. Data collection at -150°C [123(1) K], using 5 s scans/frame and 0.396° steps in ω , was performed such that a complete sphere of reflections was surveyed. This resulted in $>96.6\%$ coverage of the total reflections possible to a resolution of 0.87 Å. Cell parameters indicated a monoclinic space group. A total of 13 248 reflections were harvested from the total data collection, and final cell constants were calculated from a set of 10 422 reflections from these data. Subsequent statistical analysis of the complete reflection data set using the XPREP²² program

indicated the space group was $P2_1$. Crystal data: $\text{C}_{21}\text{H}_{20}\text{O}_6$, $a = 11.1061(2)$ Å, $b = 16.1220(2)$ Å, $c = 11.3073(2)$ Å, $V = 1824.64(5)$ Å³, $\lambda = (\text{Cu K}\alpha) = 1.54178$ Å, $\mu(\text{Cu K}\alpha) = 0.860$ mm⁻¹, $\rho_c = 1.399$ g cm⁻³ for $Z = 4$ and $M_r = 384.39$, $F(000) = 812$. After data reduction, merging of equivalent reflections, and rejection of systematic absences, 6178 unique reflections remained ($R_{int} = 0.0284$), of which 5903 were considered observed [$I_o > 2\sigma(I_o)$] and were used in the subsequent structure solution and refinement. An absorption correction was applied to the data with SADABS.³¹ Direct methods structure determination and refinement were accomplished with the SHELXTL NT ver. V6.12²² suite of programs. All non-hydrogen atom coordinates for lactone **16** were located using the default settings of that program. The remaining hydrogen atom coordinates were calculated at optimum positions using the program SHELXL.²² These latter atoms were assigned thermal parameters equal to either 1.2 or 1.5 (depending upon chemical type) of the U_{iso} value of the atom to which they were attached, and then both coordinates and thermal values were forced to ride that atom during the final cycles of refinement. All non-hydrogen atoms were refined anisotropically in a full-matrix least-squares refinement process. The final standard residual R_1 value for the model shown in Figure 3 was 0.0466 (for observed data) and 0.0477 (for all data). The corresponding Sheldrick R values were wR_2 of 0.1335 and 0.1350, respectively, and the goodness-of-fit factor was 1.052. The absolute structure parameter (Flack x parameter) = 0.1407 with esd of 0.1360. The difference Fourier map again showed insignificant residual electron density, the largest difference peak and hole being $+0.286$ and -0.554 e/Å³, respectively. The final bond distances and angles for the structural model, as shown in Figure 3, were all within acceptable limits.

Cancer Cell Line Bioassay Procedures. Inhibition of human cancer cell growth was assessed using the National Cancer Institute's standard sulforhodamine B assay as previously described.³³ Briefly, cells in a 5% fetal bovine serum/RPMI1640 medium solution were inoculated in 96-well plates and incubated for 24 h. Serial dilutions of the compounds were then added. After 48 h, the plates were fixed with trichloroacetic acid, stained with sulforhodamine B, and read with an automated microplate reader. A growth inhibition of 50% (GI_{50} or the drug concentration causing a 50% reduction in the net protein increase) was calculated from optical density data with Immunosoft software. Mouse leukemia P388 cells were incubated in a 10% horse serum/Fisher medium solution for 24 h followed by a 48 h incubation with serial dilutions of the compounds. Cell growth inhibition (ED_{50}) was then calculated using a Z1 Beckman/Coulter particle counter.

Antimicrobial Susceptibility Testing. Lignans were evaluated against the bacteria *Stenotrophomonas maltophilia* ATCC 13637, *Micrococcus luteus* Presque Isle 456, *Staphylococcus aureus* ATCC 29213, *Escherichia coli* ATCC 25922, *Enterobacter cloacae* ATCC 13047, *Enterococcus faecalis* ATCC 29212, *Streptococcus pneumoniae* ATCC 6303, and *Neisseria gonorrhoeae* ATCC 49226, and the fungi *Candida albicans* ATCC 90028 and *Cryptococcus neoformans* ATCC 90112, following established broth microdilution susceptibility assays.^{28,29} The minimum inhibitory concentration was defined as the lowest concentration of compound that inhibited all visible growth of the test organism (optically clear). Assays were repeated on separate days.

Acknowledgment. The very necessary financial assistance was provided by Outstanding Investigator Grant CA-44344-01A1-12, and Grant ROI CA-16049-01-2 from the Division of Cancer Treatment and Diagnosis, NCI, DHHS; the Arizona Disease Control Research Commission; the Fannie E. Rippel Foundation; Gary L. and Diane Tooker; the Caitlin Robb Foundation; Polly J. Trautman; Dr. John C. Budzinski; Sally Schloegel; the Eagles Art Ehrmann Cancer Fund; the Ladies Auxiliary to the Veterans of Foreign Wars; and the Robert B. Dalton Endowment Fund. Very helpful technical assistance was contributed by Drs. J. C. Knight, L. R. Landrum, D. H. Lorence, B. Orr, and J. M. Schmidt, as well as by

D. M. Carnell, F. Craciunescu, M. Dodson, L. C. Garner, C. R. Reimus, D. Nielsen Tackett, C. Weber, and L. Williams. We also wish to thank the Governments of the Republic of Maldives (M. H. Maniku, A. Naseer, and M. Shiham) and Malaysia (S. Bin Haji Abdul Majid, M. Khan Bin Momin Khan, and R. Mohamad Noordin Raja Omar) for other helpful assistance.

Supporting Information Available: Tables of X-ray crystallographic data for compounds **2**, **4–6**, and **13–16**. This material is available free of charge via the Internet at <http://pubs.acs.org>.

References and Notes

- For the preceding contribution, see: Pettit, R. K.; Fakoury B. R.; Knight, J. C.; Pettit, G. R.; Pon, S. *Antimicrob. Agents Chemother.*, submitted.
- (a) Hartwell, J. L. *Plants Used Against Cancer*; Quarterman Publications: Lawrence, MA, 1982; p 250. (b) Hata, C. *J. Chem. Soc. Jpn.* **1942**, 63, 1540–1544. (c) Yamaguchi, H.; Nakajima, S.; Arimoto, M.; Tanoguchi, M.; Ishida, T.; Inoue, M. *Chem. Pharm. Bull.* **1984**, 32, 1754–1760. (d) Tanoguchi, M.; Arimoto, M.; Saika, H.; Yamaguchi, H. *Chem. Pharm. Bull.* **1987**, 35, 4162–4168. (e) Chalandre, M.-C.; Pareyre, C.; Bruneton, J. *Ann. Pharm. Fr.* **1984**, 42, 317–321. (f) Ito, C.; Matsui, T.; Wu, T.-S.; Furukawa, H. *Chem. Pharm. Bull.* **1992**, 40, 1318–1321. (g) Gu, J.-Q.; Park, E. J.; Totura, S.; Riswan, S.; Fong, H. H. S.; Pezzuto, J. M.; Kinghorn, A. D. *J. Nat. Prod.* **2002**, 65, 1065–1068. (h) Udino, L.; Abaul, J.; Bourgeois, P.; Corrichon, L.; Duran, H.; Zedde, C. *Planta Med.* **1999**, 65, 279–281. (i) Dittmar, A. *J. Ethnopharmacol.* **1991**, 33, 243–251. (j) Yakushijin, K.; Sugiyama, S.; Mori, Y.; Murata, H.; Furukawa, H. *Phytochemistry* **1980**, 19, 161–162. (k) Chen, I.-S.; Chen, J.-J.; Duh, C.-Y.; Tsai, I.-L.; Chang, C.-T. *Planta Med.* **1997**, 63, 154–157. (l) Chen, J.-J.; Tsai, I.-L.; Chen, I.-S. *J. Nat. Prod.* **1996**, 59, 156–158. (m) Chen, I.-S.; Chen, J.-J.; Duh, C.-Y.; Tsai, I.-L. *Phytochemistry* **1997**, 45, 991–996. (n) Masuda, T.; Oyama, Y.; Yonemori, S.; Takeda, Y.; Yamazaki, Y.; Mizuguchi, S.; Nakata, M.; Tanaka, T.; Chikahisa, L.; Inaba, Y.; Okada, Y. *Phytother. Res.* **2002**, 16, 353–358.
- Shibata, S.; Murata, T.; Fujita, M. *Yakugaku Zasshi* **1962**, 82, 777–779.
- Forsey, S. P.; Rajapaksa, D.; Taylor, N. J.; Rodrigo, R. *J. Org. Chem.* **1989**, 54, 4280–4290.
- Nishino, C.; Mitsui, T. *Tetrahedron Lett.* **1973**, 14, 335–338.
- Matsui, K.; Wada, K.; Munakata, K. *Agric. Biol. Chem.* **1976**, 40, 1045–1046.
- Ichino, K.; Tanaka, H.; Ito, K. *Phytochemistry* **1988**, 27, 1906–1907.
- Richomme, P.; Bruneton, J.; Cave, A. *Heterocycles* **1985**, 23, 309–312.
- Yamaguchi, H.; Arimoto, M.; Yamamoto, K. O.; Numata, A. *Yakugaku Zasshi* **1979**, 99, 674–677.
- McDoniel, P. B.; Cole, J. R. *J. Pharm. Sci.* **1972**, 61, 1992–1994.
- Nishibe, S.; Hisada, S.; Inagaki, I. *Yakugaku Zasshi* **1974**, 94, 522–524.
- Takaoka, D.; Takamatsu, N.; Saheki, Y.; Kono, K.; Nakaoka, C.; Hiroi, M. *Nippon Kagaku Kaishi* **1975**, 12, 2192–2196.
- Koul, S. K.; Taneja, S. C.; Dhar, K. L.; Atal, C. K. *Phytochemistry* **1983**, 22, 999–1000.
- Nishibe, S.; Chiba, M.; Hisada, S. *Yakugaku Zasshi* **1977**, 97, 1366–1369.
- Mikaya, G. A.; Turabelidze, D. G.; Kemertelidze, E. P.; Zaikin, V. G.; Vul'fon, N. S. *Bioorg. Khim.* **1980**, 6, 1415–1419.
- Zhao, C.; Nagatsu, A.; Hatano, K.; Shirai, N.; Kato, S.; Ogihara, Y. *Chem. Pharm. Bull.* **2003**, 51, 255–261.
- Yamamoto, D.; Ohishi, H.; Kozawa, M.; Inamori, Y.; Ishida, T.; Inoue, M. *Chem. Pharm. Bull.* **1988**, 36, 3239–3247.
- Tomioka, K.; Ishiguro, T.; Litaka, Y.; Koga, K. *Tetrahedron* **1984**, 40, 1303–1312.
- Billups, W. E.; Blakeney, A. J.; Chamberlain, W. T. *J. Org. Chem.* **1976**, 41, 3722–3773.
- Nishibe, S.; Okabe, K.; Hisada, S. *Chem. Pharm. Bull.* **1981**, 29, 2078–2082.
- Nishibe, S.; Fujimoto, T.; Nose, M.; Takada, T.; Ogihara, Y.; Xu, G. *Phytochemistry* **1993**, 32, 1579–1581.
- SHELXTL-NT-Version 6.12, an integrated suite of programs for the determination of crystal structures from diffraction data; Bruker AXS, Inc.: Madison, WI, 2001. This package includes, among others, XPREP (an automatic space group determination program), SHELXS (a structure solution program via Patterson or direct methods), and SHELXL (structure refinement software).
- Tables of X-ray crystallographic data (98 pages) for compounds **2**, **4–6**, and **13–16** are available free of charge via the Internet at <http://pubs.acs.org>. This crystallographic data has also been deposited with the Cambridge Data Centre. Copies of the data can be obtained, free of charge, on application to the Director, CCDC, 12 Union Rd., Cambridge CB2 1EZ, UK [fax: +44(0)1223-336033 or e-mail: deposit@ccdc.cam.ac.uk].
- (a) Cambie, R. C.; Craw, P. A.; Rutledge, P. S.; Woodgate, P. D. *Aust. J. Chem.* **1988**, 41, 897–918. (b) Buckleton, J. S.; Cambie, R. C.; Clark, G. R.; Craw, P. A.; Rickard, C. E. F.; Rutledge, P. S.; Woodgate, P. D. *Aust. J. Chem.* **1988**, 41, 305–324.
- Kim, Y.; Kim, S. B.; You, Y. J.; Ahn, B. Z. *Planta Med.* **2002**, 68, 271–274.
- Ito, C.; Itoigawa, M.; Ogata, M.; Mou, X. Y.; Tokuda, H.; Nishino, H.; Furukawa, H. *Planta Med.* **2001**, 67, 166–168.
- Lim, Y. H.; Leem, M. J.; Shin, D. H.; Chang, H. B.; Hong, S. W.; Moon, E. Y.; Lee, D. K.; Yoon, S. T.; Woo, W. S. *Arch. Med. Res.* **1999**, 22, 208–212.
- National Committee for Clinical Laboratory Standards 2000. Methods for dilution antimicrobial susceptibility tests for bacteria that grow aerobically. Approved standard M7-A5, NCCLS, Wayne, PA, 2000.
- National Committee for Clinical Laboratory Standards 2002. Reference method for broth dilution antifungal susceptibility testing of yeasts. Approved standard-second edition, M27-A2, NCCLS, Wayne, PA, 2002.
- Bligh, E. G.; Dyer, W. J. *Can. J. Biochem. Physiol.* **1959**, 37, 911–917.
- Blessing, R. *Acta Crystallogr.* **1995**, A51, 33–8.
- (a) Ward, R. S.; Hughes, D. D. *Tetrahedron* **2001**, 57, 4015–4022. (b) Landais, Y.; Robin, J.-P.; Lebrun, A. *Tetrahedron* **1991**, 47, 3787–3804. (c) Landais, Y.; Robin, J.-P. *Tetrahedron Lett.* **1986**, 27, 1785–1788. (d) Damon, R. E.; Schlessinger, R. H.; Blount, J. F. *J. Org. Chem.* **1976**, 41, 3772–3773. (e) Kupchan, S. M.; Dhingra, O. P.; Kim, C. K.; Kameswaran, V. *J. Org. Chem.* **1976**, 41, 4047–4049. (f) Kupchan, S. M.; Dhingra, O. P.; Kim, C. K. *J. Org. Chem.* **1976**, 41, 4049–4050. (g) Ward, R. S. *Nat. Prod. Rep.* **1993**, 10, 1–28.
- Monks, A.; Scudiero, D.; Skehan, P.; Shoemaker, R.; Paul, K.; Vistica, D.; Hose, C.; Langley, Jr.; Cronise, P.; Vaigro-Wolff, A. *J. Natl. Cancer Inst.* **1991**, 83, 757–766.

NP030125S